JTTEE5 19:1100–1114
DOI: 10.1007/s11666-010-9513-0
1059-9630/$19.00 © ASM International

Study of the Splat Microstructure and the Effects of Substrate Heating on the Splat Formation for Ni-Cr Particles Plasma Sprayed onto Stainless Steel Substrates

S. Brossard, P.R. Munroe, A.T. Tran, and M.M. Hyland

(Submitted January 19, 2010; in revised form April 20, 2010)

The plasma spraying process is still poorly understood in term of the processes by which the coating is built up, especially coating interactions with the substrate. This present study enhances this understanding by studying, through a range of electron microscopy techniques, single NiCr splats plasma sprayed onto stainless steel substrates, which were first exposed to different heat treatments. The microstructure of the splats, particularly the splat-substrate interface, was characterized, and the formation of the observed features is discussed. Evidence of localized substrate melting and inter-mixing with the splat material was found, showing metallurgical bonding. The structures observed were also correlated to the treatment of the substrate, demonstrating how such treatments can influence the properties of the fully deposited coating by modifying the splat formation process. Most notably, heating the substrate during spraying was found to significantly modify splat formation by reducing splashing and increasing the extent of substrate melting.

Keywords interface, nickel chromium, oxide, plasma spray, splat, stainless steel

1. Introduction

Conventional plasma spraying is one of the most commonly used thermal spray processes due to its flexibility and versatility, allowing the manufacturing of coatings made of almost any material with a congruent melting point onto a wide range of ceramic, metallic, or polymer substrates. Such a process permits the substrates to retain their original characteristics (chemistry, structure, and properties), as they undergo no or minimal melting. Further, it avoids the use of potentially polluting chemical solutions. However, understanding of the mechanisms of interaction between substrate and coating and the nature of their interface is limited for many thermal spray processes (Ref 1, 2).

Coatings are made through the accumulation of the sprayed molten particles which flatten upon impact to form lamella, often termed splats. The microstructure of fully deposited coatings has been studied through the observation of cross sections at both a macroscopic and microscopic level (Ref 3-6). However, for a more detailed insight of the coating formation process and the nature of the splat interaction with the substrate, study of single splats is necessary and a number of prior studies have been performed which have investigated these features. Morphology of the splats has also often been observed at both a macroscopic level (with millimeter size droplets, allowing in situ study of their formation (Ref 7-11)) and microscopic level (with micron size droplets) (Ref 12), to understand the influence of factors such as the spray conditions, the combination of materials used as substrate and feedstock powder (Ref 13, 14), the temperature of the substrate during spraying (Ref 3, 14-19) or the substrate surface topography and chemistry (Ref 7, 16, 20-23). For example, it was observed that substrate temperature during spraying was a key parameter for the control of splashing of the splats. Specifically, for substrates heated above a particular temperature, termed the ''transition temperature'', disk-shaped splats were obtained, instead of very irregularly shaped splats (Ref 3, 14-18). Possible explanations for such phenomenon include desorption upon heating of adsorbates/condensates that were initially present on the substrate surface, and the solidification of the splat starting during flattening.

There have been relatively fewer published studies that have focused on the coating-substrate interface. Kitahara et al., studied the coating-substrate interface by spraying a range of materials including Ni and Cr, onto various

S. Brossard and **P.R. Munroe**, School of Materials, University of New South Wales, Sydney, NSW 2052, Australia; and **A.T. Tran** and **M.M. Hyland**, Chemical & Materials Engineering Department, University of Auckland, Auckland 1142, New Zealand. Contact e-mail: sophie.brossard@student.unsw.edu.au.

substrates including mild steel (Ref 24). They observed, by x-ray diffraction, in most cases, the presence of an intermetallic layer at the interface, interpreted as evidence of localized substrate melting. However, such interactions were not observed for the case of either Ni or Cr sprayed onto steel substrates. Localized steel substrate melting was also observed by Zhang et al. (Ref 14) and by Li et al. (Ref 25), both when plasma spraying Mo. In this case, a Fe_2Mo intermetallic phase was observed by transmission electron microscopy (TEM) at the interface. In such cases, bonding between the coating and substrate is said to be metallurgical. Elsewhere, the adhesion of the coating is expected to occur by mechanical interlocking (Ref 1), as substrate melting has either not been investigated or directly observed (Ref 21, 23, 26-28).

Modeling has also been widely used to describe the splat formation process (Ref 9, 29, 30). However, such models cannot explain all the features observed, such as localized substrate melting, possibly due to the lack of precise input data and the difficulty of modeling discontinuous, non-averaged, heat transfer resistance across the interface.

Indeed, very little work on splat microstructure and the splat-substrate interface at high resolution has been performed. In the present study, particles of NiCr, a material often used in thermal sprayed coatings as bond coat or for protection of steel against heat, corrosion (Ref 31), erosion, for example in boilers (Ref 1), were plasma sprayed to form single splats. The substrates used were 304 stainless steel and subjected to different heat treatments, i.e., sprayed at room temperature as-polished, sprayed at room temperature after being heat-treated, and heated during spraying. Such treatments are expected to vary the substrate's surface chemistry, which may in turn influence the splat formation process and their final morphology. Indeed, as noted earlier, heating the substrate during spraying may significantly reduce splashing upon splat formation (Ref 3, 14-18). Furthermore, NiCr or Ni splats formed on pre-heat treated steel specimens were found to be much flatter, with a larger diameter (Ref 7, 32). Cedelle et al. suggested this was possibly due to a better wetting from the Ni splat, supposedly from the positive skewness resulting from the heat treatment (Ref 7), which increases the oxide content of the substrate surface (Ref 33).

Previous studies, by the same authors as this present publication, have described the microstructure of plasma sprayed NiCr splats on steel substrates which had first undergone various pre-treatments (as-polished, thermally treated, boiled, boiled and thermally treated etc.) (Ref 32, 34). Evidence of localized substrate melting was observed, as well as an increase in splat diameter for both heated and boiled specimens. It was also noted that pre-heating the substrate prior to spraying significantly reduced the occurrence of substrate melting, possibly because the splats were also noted to be thinner. However, compared to the work presented here, spraying conditions were significantly different (that is, both the velocity and temperature of the sprayed particles were notably lower). As a result, the morphologies of the splats in this study were significantly different from those observed in prior studies. Moreover, particles were also sprayed onto heated substrates in this study, whereas prior research as restricted to substrates held at room temperature.

The NiCr single splats formed on the steel substrates (sprayed as-polished, after thermal treatment or heated during spraying) were studied using a range of electron microscopy techniques, to investigate their microstructure and their interaction with the substrate. Observations were then used to discuss the effects of substrate surface chemistry induced by heat treatments and the splat formation process.

2. Experimental Procedure

Three different substrates were used; all prepared from stainless steel 304. These are listed in Table 1.

All substrates were first mechanically ground and mirror polished with diamond paste, to a nanoscale roughness. The thermally treated substrate was heated at 350 °C for 90 min in air. Such a treatment is expected to increase the oxide content of the substrate surface, partially dehydrate the oxide layers, and/or to induce some level of surface roughness. Moreover, it was performed several hours prior to spraying, meaning that some adsorbates/condensates, notably moisture for the air, can reform on the substrate surface. One substrate was also heated to a temperature of 350 °C 30 min before spraying, and then hold at that temperature during spraying, which is above the expected transition temperature at which adsorbates/condensates species, such as water, present on the substrate surface may be released (Ref 33).

The sprayed material was a commercial NiCr alloy powder (Ni80-Cr20, Sulzer Metco 43 VF-NS, Switzerland, (−106 + 45) μm). Plasma spraying was carried out with a Sulzer Metco (Switzerland) 7MB gun (with a nozzle diameter of 8 mm), operating at a current of 550 A and at a voltage of 62 V, with a spraying distance of 100 mm. The feeding rate of the powder was of 1 g/min, the carrier gas being argon at a flow rate of 3 SLPM, while the plasma gas was a mixture of nitrogen and hydrogen, at a flow rate of 47.5 and 6.2 SLPM, respectively.

The specimens were then characterized using a range of analytical techniques. A Hitachi S3400 scanning electron microscope (SEM) was used to image the overall morphology of the splats and the substrates. A FEI xP200 Focused Ion Beam microscope (FIB) was used to mill cross sections of the splats using an energetic gallium ion beam, and to image them using secondary electrons induced by the ion beam. Details have been described elsewhere (Ref 35). A FEI xT Nova Nanolab 200 dual

Table 1 Substrate nomenclature and condition

Specimen	Substrate	Pre-treatment
SS_P	Stainless steel	Polished (to a nanoscale smoothness)
SS_PT	Stainless steel	Polished and thermally treated prior to spraying
SS_PH	Stainless steel	Polished and heated during spraying

beam microscope (that is a FIB and SEM combined into a single instrument) was used to prepare cross sections of splats (100-200 nm in thickness) suitable for TEM observation. These were prepared using the lift-out method as described elsewhere (Ref 35) and examined in a Philips CM200 transmission electron microscope (TEM) to which energy dispersive x-ray spectroscopy (EDS) facilities have been interfaced. Finally, the average surface roughness of the substrates was measured using a Digital Instruments DI3000 Atomic Force Microscope (AFM).

Several FIB and TEM cross sections were prepared and studied for each particular feature and/or type of splat. However, for reasons of brevity only a small number of representative images will be presented here. The cross section preparation process using FIB also involves the deposition of a layer of platinum on top of it prior to milling for protection purposes. This layer is present on the FIB and TEM images presented.

3. Results and Discussion

Observations concerning the morphology of the splats, their microstructure and the splat-substrate interface, as observed on FIB and TEM cross sections, are detailed, and the splat formation discussed, firstly for the polished (SS_P) and polished and thermally treated (SS_PT) specimens, as they are quite similar, then secondly, for the substrates heated (SS_PH) during spraying.

3.1 Study of the Splats Found on the SS_P and SS_PT Substrates

3.1.1 Description of the Splat Population. SEM images of about 50-60 splats were recorded for both substrate types. For each splat, the diameter, D, was evaluated by measuring the smallest and largest values and taking the average, D_m. Splashed fingers were ignored. However, for splats presenting a dense ring of splashed fingers, the diameter, D_r, for this ring was also measured and expressed as a function of the diameter of the splat itself. See Fig. 1(a) for example.

Three types of splats were recognized:

- Splats presenting a large and dense ring of splashed fingers (see SEM image presented Fig. 1a). Such splats were denoted ''RSF splats''.
- Splats with no splashed fingers (Fig. 1b). Such splats were denoted ''NSF splats''.
- Very fragmented splats (Fig. 1c).

The relative population and dimensions of the splats found on the SS_P and SS_PT specimens are summarized in Table 2. It can be noted that the RSF splats represent the majority of the splats observed, but their diameter is smaller, possibly because of the material loss from the splashing. A detailed comparison between the values from the non-thermally treated and the thermally treated specimen is given later and provides an understanding of the effects of such a thermal treatment.

3.1.2 Structure and Formation of the RSF Splats. Figure 2 shows a TEM cross section made across the central part of such splat found on SS_P (the inset secondary electron image shows both the splat and the location of the cross section). Firstly, it can be observed that toward the center of the splat, the splat-substrate interface (marked 1) is indistinct and the grains boundaries of the steel and NiCr phases are coincident across this interface (marked 2). The EDS elemental linescan, marked L1 (Fig. 2d), performed across this part of the

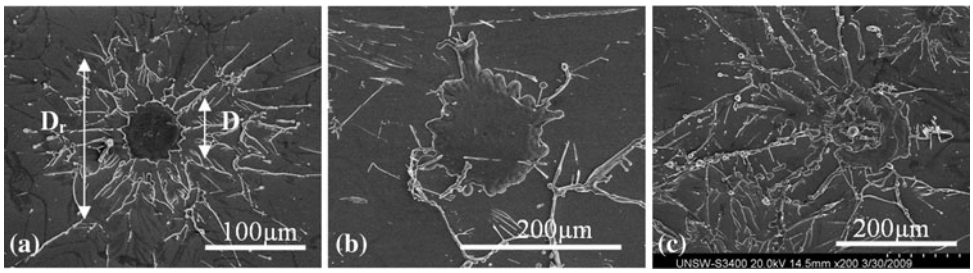

Fig. 1 SEM images of different types of splats found on SS_P and SS_PT: (a) splat with a ring of splashed fingers, (b) splat with no splashed fingers, (c) very fragmented splat with splashed fingers

Table 2 Relative proportions and average diameter of the splats (and average diameter of the ring of splashed fingers if applicable) found on SS_P and SS_PT

	SS_P		SS_PT	
RSF splats	44%	$D_m = [81 \pm 30]$ µm $D_r = [3.0 \pm 0.8]$ D	60%	$D_m = [135 \pm 45]$ µm $D_r = [2.2 \pm 0.6]$ D
NSF splats	39%	$D_m = [95 \pm 38]$ µm	40%	$D_m = [161 \pm 80]$ µm
Very fragmented splats	17%	$D_m = [104 \pm 30]$ µm $D_r = [2.3 \pm 0.8]$ D	…	

interface shows that the variation of Ni and Fe concentrations is gradual (3): interdiffusion of both elements has occurred over a distance of about 200 nm. Electron diffraction studies, particularly the observation of Kikuchi maps, also showed that on each side of the interface the grains exhibit the same orientation. Both NiCr and austenitic stainless steel have the same crystal structure (face-centered cubic), with similar lattice parameter (0.352 nm for steel, 0.355 nm for NiCr). It can be concluded that, contrary to previous studies (Ref 24), localized melting of the substrate has occurred, allowing the interdiffusion of both phases over a significant depth, but no intermetallic phase was observed to be present. Furthermore, the Fe and Ni EDS elemental maps (Fig. 2b and c) show that the substrate has jetted within the NiCr splat (4) in a way that clearly indicates the steel substrate has been melted. The occurrence of steel melting is consistent with modeling experiments which have shown that temperature at the splat-substrate interface may reach 1660 °C, the melting point of steel being 1454 °C (Ref 36). This would, however, require intimate contact between the molten splat and the substrate.

The grains of the splat, which here are columnar, have thus formed epitaxially on the pre-existing grains of the steel substrate. It was also observed that in such a location where very good contact between splat and substrate is achieved and substrate melting has occurred, that the grains are relatively large (up to 10 μm in diameter, compared to 1-2 μm in other regions where melting did not occur). This suggests that solidification in this region was relatively slow, which is unexpected considering that intimate contact between splat and substrate usually implies efficient heat removal from the splat through the interface with the substrate. The fact that the thermal diffusivity of steel (~4×10^{-5} m^2/s^1, as calculated from Ref 37) is relatively low compared to other metals may have played a role in retaining the heat and slowing the solidification process.

Some voids may also be found in the center of such splats, as it can be seen on the FIB cross section presented in Fig. 3(a) (region marked 1). It can be noted that they are not located at the splat-substrate interface, but rather within the splat itself. The splat-substrate interface (2) is also indistinct and irregular, evidence that melting of the substrate has occurred at this location, along with some mixing/interdiffusion between the NiCr and steel phases, while some grains boundaries (3) are coincident across the interface.

The intimate contact between the splat and substrate and the observation of substrate melting are not evident on all splats with this morphology or even all along a single splat. As it can be seen on the FIB cross sections in Fig. 3, under the rim of the splats (Fig. 3b) or under the

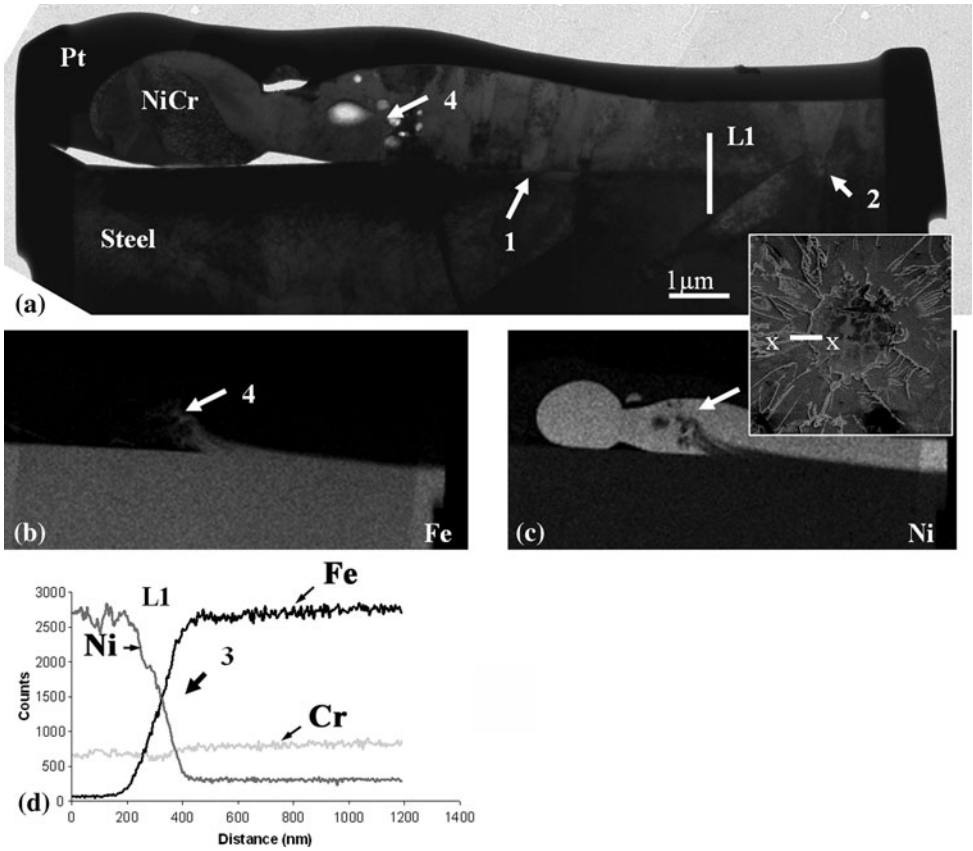

Fig. 2 TEM cross section made across the rim of a RSF splat (see insert picture) found on SS_P: (a) bright field image, EDS elemental maps for (b) Fe, (c) Ni, (d) EDS elemental linescan

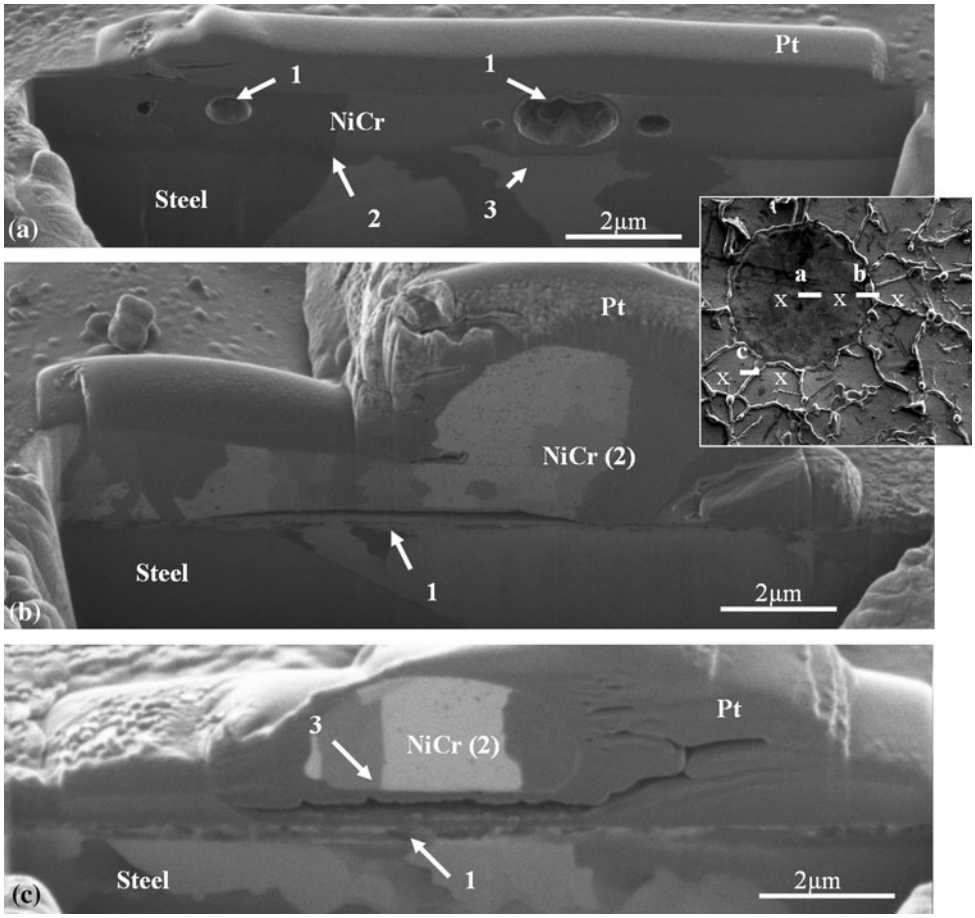

Fig. 3 FIB cross section made across (a) the center, (b) the rim, (c) a splashed finger of a RSF splat (see insert picture) found on SS_P

splashed fingers of the splat (Fig. 3c), the contact between splat and substrate is always poor. Here, the outer surface of the substrate is clearly visible and flat (1), no evidence of substrate melting can be found, while the grains of the splat are coarse and irregular (2) rather than columnar (with diameters ranging from 1 to 5 μm). This is consistent with poor contact, as it shows that significant thermal contact resistance, induced by the gap present between the splat and the substrate, has prevented efficient heat removal from the splat through the substrate, inducing a relatively slow rate of solidification.

Iron oxide was often found to have formed on the lower surface of the splats where they have been lifted-up away from the substrate, notably under the rim or the splashed fingers of the splats, as it can be seen for instance on Fig. 3(c) (3). This phase has been identified by TEM as being wustite (FeO). Such an oxide phase may have formed from iron that has deposited on the bottom surface of the splat and became oxidized by the hot oxidizing gases that may be present here (see section 3.1.4 for more detail on their formation) when the splat becomes lifted-up. Wustite may have formed in preference to other forms of iron oxide possibly due to the limited supply of oxygen, as it is located in an enclosed space. Figure 4 shows a TEM cross section made across a splashed finger: EDS elemental maps (Fig. 4b, d, and e) show that such a phase contains Fe, Cr, and O (1), and the rings obtained from the diffraction pattern (presented Fig. 4f) are consistent with being from spinel $FeO{\cdot}Cr_2O_3$, which is another oxide form that can form, in a similar manner to FeO (Ref 38, 39).

Some splats, found on the thermally treated substrate, SS_PT, also display a distinct splat-substrate interface in their center, such as that seen on the TEM cross section presented Fig. 5(a) (1). The linescan L1 (Fig. 5) confirms the absence of interdiffusion between Ni and Fe across the interface, as the variation of their concentrations is sharp at the interface (2). In such locations, grains are usually columnar and relatively large (5-10 μm) (3), similar to the splats where substrate melting has occurred, as described earlier.

Furthermore, the Cr EDS elemental map (Fig. 5d) and the linescan (Fig. 5e) show that a thin layer of chromium has segregated to the splat-substrate interface (4), and it is most probable that this phase is chromium oxide. Such an oxide may have formed from the oxidation of the chromium in the steel substrate, either from the heat treatment (as this is only found on the thermally treated specimen), or from the heat provided by the plasma flame. The layer of oxide is too thin to be unambiguously identified by electron diffraction, however, previous studies of the

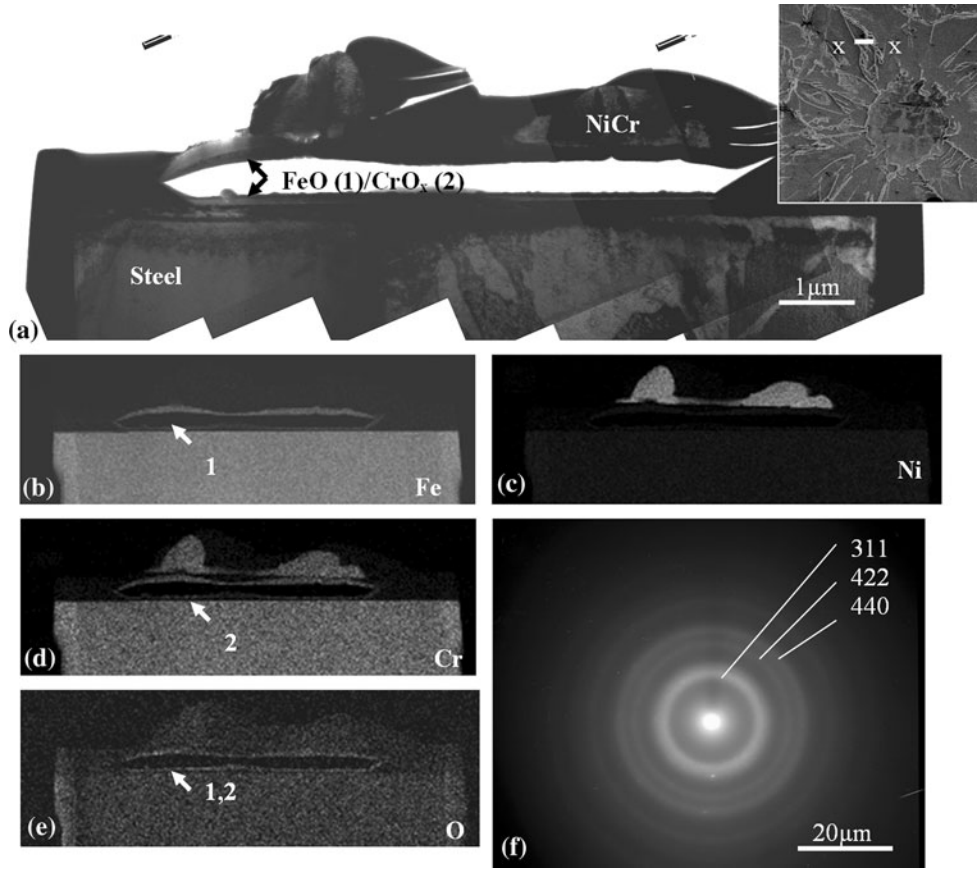

Fig. 4 TEM cross section made across a splashed finger of a RSF splat (see insert picture) found on SS_P: (a) bright field image, EDS elemental maps for (b) Fe, (c) Ni, (d) Cr, (e) O, (f) spinel $FeO{\cdot}Cr_2O_3$ diffraction pattern

oxidation of stainless steel showed that Cr_2O_3 was the species most likely to form on stainless steels, such as the 304 type, along with Fe_2O_3 and associated spinel oxides (Ref 38, 39).

3.1.3 Structure and Formation of the NSF Splats and Very Fragmented Splats. Despite their difference in shape, both categories of splats displayed the same general features regarding their interaction with the substrate. Indeed, it was frequently found that the contact between splat and substrate was poor, such as on the left side of the TEM cross section shown Fig. 6 (1), where FeO is present on the underside of the splat (2) as a relatively thick (50-200 nm) and dense layer. In some zones, however, good contact between splat and substrate is achieved (3); the interface remains distinct in most cases, thus with no obvious evidence of substrate melting. However, as shown on the linescan L1 (Fig. 6f) performed across the interface, interdiffusion between Ni and Fe may occur, in this instance over a depth of about 100 nm (4).

Substrate melting was not common, but it was observed in some instances, as shown for example on the TEM cross section shown in Fig. 7: on the EDS elemental maps (Fig. 7b and c) it can be seen that some steel has been jetted within the splat (1), while the splat-substrate interface is also indistinct (Fig. 7a, 2).

Oxide formation is, however, much more common for these splats. Apart from iron oxide, as described previously, chromium oxide was found in larger amounts compared to the RSF splats. Indeed, it may be observed as a dense layer on the outer surface of the splat, as seen in Fig. 6 (5) on the bright field image (Fig. 6a) and on the Cr and O EDS elemental maps (Fig. 6d and e). Where the layer was thick enough, electron diffraction allowed the identification of this phase as Cr_2O_3. An example of a diffraction pattern is shown in Fig. 6(g). It can be seen that the pattern consists of poorly defined rings, due to the fine grained structure (a few 10 nm) of the oxide, Cr_2O_3. This oxide has been shown to be the most probable species of chromium oxide to form from the oxidation of NiCr alloys (Ref 40, 41). Cr_2O_3 was also found at the splat-substrate interface, see Fig. 8, and present at the center of a very fragmented splat. It is present here as a significantly thick layer, marked 1 on the bright field image (Fig. 8a) and the EDS elemental maps (Fig. 8d and e). However, while the formation of chromium oxide on the outer surface of the splat may be expected, the presence of such thick layer (100-200 nm) of oxide at the splat-substrate interface is less obviously understood. Indeed, the layer appears too thick to have formed from the oxidation of the stainless steel substrate only, as studies have shown that such layers

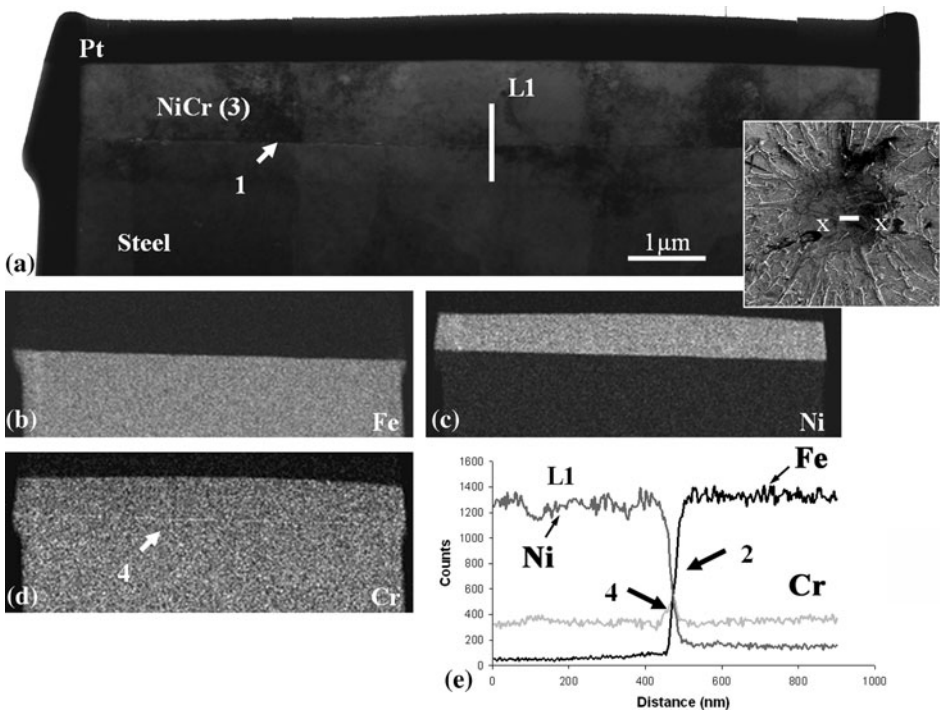

Fig. 5 TEM cross section made across the center of a RSF splat (see insert picture) found on SS_PT: (a) bright field image, EDS elemental maps for (b) Fe, (c) Ni, (d) Cr, (e) EDS elemental linescan

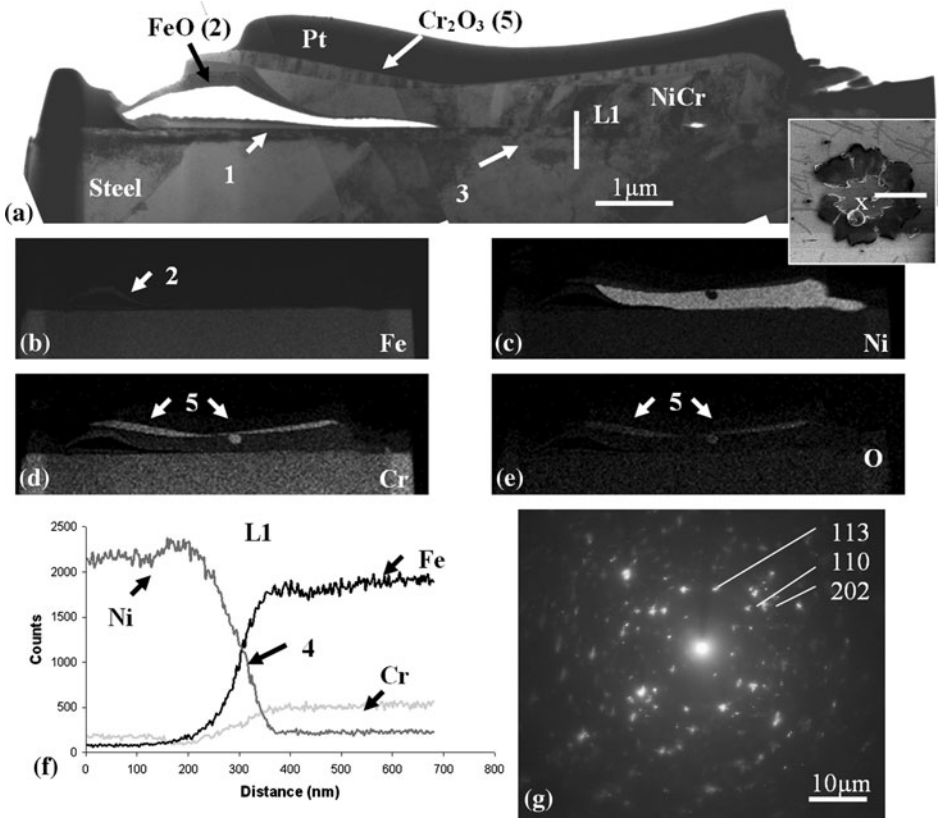

Fig. 6 TEM cross section made across a NSF splat (see insert picture) found on SS_P: (a) bright field image, EDS elemental maps for (b) Fe, (c) Ni, (d) Cr, (e) O, (f) elemental linescan, (g) Cr_2O_3 diffraction pattern

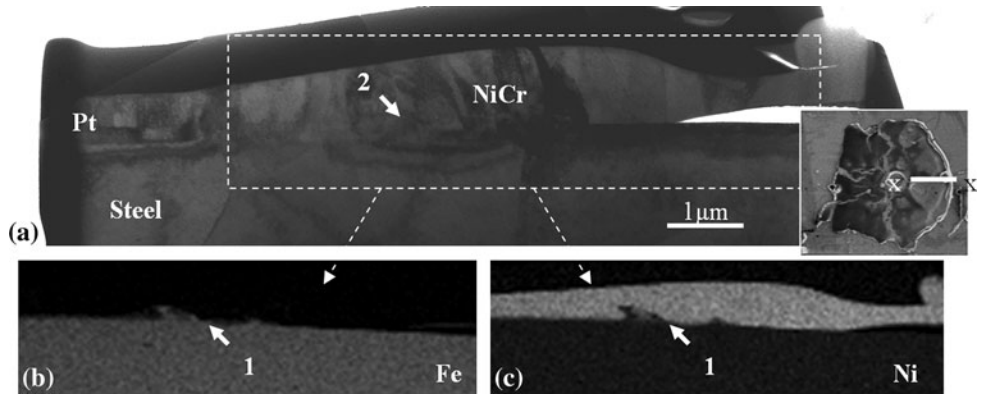

Fig. 7 TEM cross section made across a NSF splat (see insert picture) found on SS_P: (a) bright field image, EDS elemental maps for (b) Fe, (c) Ni

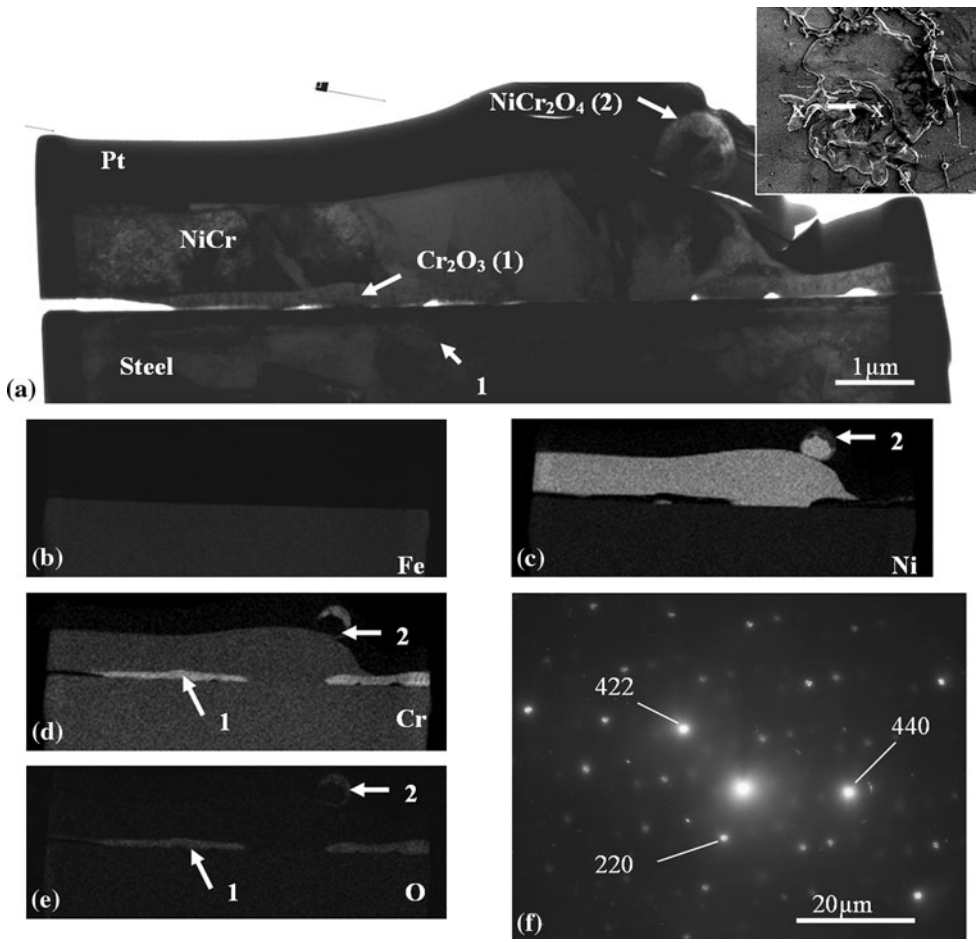

Fig. 8 TEM cross section made across the center of a NSF splat (see insert picture) found on SS_P: (a) bright field image, EDS elemental maps for (b) Fe, (c), Ni, (d) Cr, (e) O, (f) $NiCr_2O_4$ diffraction pattern

are usually both uniform and only a few nanometers thick (Ref 38, 39). It has presumably formed from oxidation of the splat. In-flight oxidation of the particle has been shown to lead to the formation of Cr oxide (Ref 3), and thus may be the cause of the layer of oxide observed here. Otherwise, such an oxide may have formed after impact due to the presence of significant amounts of hot oxidizing gases, as noted in previous studies of splat formation (Ref 3, 15, 32, 42) where there is evidence of gas release from the substrate upon impact and spreading of the particle.

On the same cross section presented in Fig. 8, spinel $NiCr_2O_4$ (2) was also identified by EDS elemental mapping (Fig. 8c to e) and electron diffraction (see corresponding diffraction pattern presented at Fig. 8f). This phase, along with NiO (which was not observed on this section), is generally expected to form during the oxidation of NiCr alloys (Ref 40, 41), and was also found to form in previous microstructural studies of NiCr splats formed on steel (Ref 32, 34), but in those studies these phases were observed more frequently. Such differences may be linked to differences in the splat morphology (splats observed in the previous study did not display as many splashed fingers), possibly caused by variations in the spray conditions and substrate preparation conditions.

3.1.4 Summary of the Splat Formation Processes. In the plasma spray process, the particles impact the substrate in a fully molten state. Many previous studies have investigated how, upon particle impact, adsorbates/condensates become released from the substrate surface, creating instabilities leading to splashing (Ref 3, 15, 32, 42). The numerous splashed fingers observed around the majority of the splats indicate this occurs here. Consequently, for the RSF splats, the formation process may be summarized as follows: upon impact and flattening of the molten NiCr particle, adsorbates/condensates are released from the substrate, and pushed outwards by the flowing NiCr (as no or few voids have been observed toward the center of the splats previously described). Splashing occurs, possibly partly due to the instability created by the presence of the desorbed species, some molten material gets jetted away from the substrate, forming the fingers observed. Moreover, a potential correlation with the occurrence with substrate melting may be noted. Splats which exhibited no evidence of substrate melting and inter-mixing had few splashed fingers. The plasma sprayed splats studied in previous publications (Ref 32, 34) also revealed limited substrate melting and fewer splashed fingers. Finally, impact splashing, as described for example by Escure et al. (Ref 43) and Cedelle et al. (Ref 8), may also have occurred. Small NiCr droplets may then be splashed away and, when falling back on the substrate, form very small NiCr fragments (usually less than a few microns in size) that were not counted as splats.

In the central part of the splat, good contact with the substrate is achieved due to the pressure applied by the particle on impact on the substrate. This is where the heat transmitted from the molten splat to the substrate may cause local melting. Interdiffusion occurs between the splat and substrate and slow solidification of the molten material, then forming large columnar grains, take place. However, in some cases melting of the substrate may not be achieved. As will be discussed shortly, this is believed to be an effect of the thermal treatment applied to the substrate prior to spraying. Toward the periphery and the splashed fingers, the pressure applied by the splat on the substrate is insufficient to allow good adhesion between splat and substrate, or substrate melting. Consequently, when the splat solidifies and cools, curling up of the splat takes place as a means to accommodate thermal stress (Ref 44). Some iron from the substrate may become attached to the bottom splat of the splat where it is lifted-up and this becomes oxidized, forming FeO layers.

For the very fragmented splats, an explanation of their shape would be that the species desorbed from the substrate are sufficient to create instabilities which are able to cause the breaking up of the flattening molten splat. Consequently, good contact between splat and substrate may not be achieved in the central part of the splat, and no substrate melting may occur.

Finally, for the NSF splats, it is not well understood why splashing was limited. Presumably, fewer adsorbates/condensates may have been released from the substrate, limiting the splashing. However, this would not explain why either no or limited substrate melting was observed, even on the non-heat treated specimen.

3.1.5 Effects of the Thermal Treatment Prior to Spraying. As explained in the introduction, the effects of thermally treating stainless steel substrates before plasma spraying NiCr particles have been investigated in a previous study (Ref 32). Overall, the trends observed were similar with the ones obtained here. Indeed, for both studies, splats on the heat-treated substrates, compared to the non-heat-treated surfaces, display larger diameters. This can be seen here in Table 2. Possible explanations include the increase in the skewness of the surface of the substrate (because of the increase in the oxide content of the surface (Fe_2O_3 and Cr_2O_3)) so it becomes positive, which improved the wettability of the molten splat on the substrate (Ref 7). Also, evidence of substrate melting was less common for the thermally treated substrates, possibly because the splats were flatter, thus transmitting less heating per unit of area to the substrate, or the increase in oxide content increased the thermal resistance.

It should be noted that the effects of pre-heat treatment (increase in splat flattening and decrease in the occurrence of substrate melting) are similar between both studies despite the significant difference in the splats shapes. Thus, for more details on such effects of pre-heat treatment, one should refer to the previous publication (Ref 32).

It should also be noted that the relative proportion of NSF splats remained unchanged on heat-treatment of the substrate. On the other hand, after such treatment, there are no fragmented splats, rather larger, more regularly shaped RSF splats. As discussed previously, the heat treatment may, at least partially, dehydrate the substrate surface layers, thus limiting the amount of species which get desorbed upon splat formation, which would then be insufficient to cause the break-up of the sprayed particle. The better wetting induced by the heat-treatment may also play a role.

To conclude, the occurrence of substrate melting is beneficial as it means that the bonding between splat and substrate is metallurgical in these areas. However, it occurs only in limited areas of only a portion of the splats. Elsewhere some voids, including those formed from splat curl-up, and oxides may be detrimental to the properties of the full deposited coating. Heat-treatment of the substrate before spraying, results in a reduction of the occurrence of substrate melting, which may be subsequently unfavorable to the coating's adhesion strength.

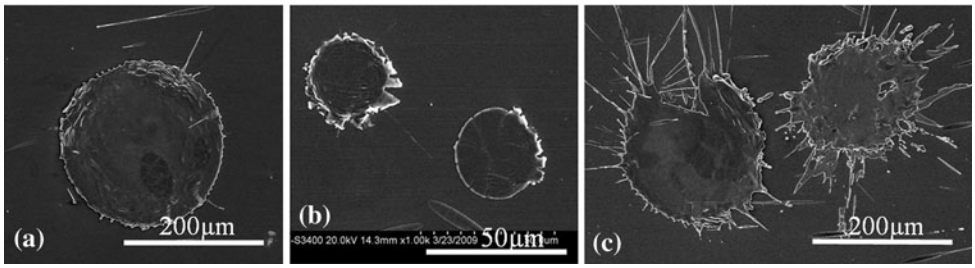

Fig. 9 SEM images of the different types of splats found on SS_PH: (a) large circular splat, (b) small circular splat, (c) irregularly shaped splat

3.2 Study of the Splats Found on the SS_PH Substrate

3.2.1 Description of the Microstructure and Formation of the Splats. As it can be seen on the SEM images displayed in Fig. 9, the splats found on the SS_PH substrate exhibited a very different morphology compared to the substrates held at room temperature during spraying (thus, they are described separately). Indeed, the large majority of splats are disk-shaped, with a smooth rim (see Fig. 9a and b). However, a bimodal distribution was observed and the splats can be divided into two different types: large circular splats (~45% of the total splat population with an average diameter $D_m = [210 \pm 78]$ μm, see Fig. 9a), and small circular splats (~46%, $D_m = [37 \pm 13]$ μm, Fig. 9b). In addition to this, some large splats were also found to exhibit a relatively irregularly shaped rim with short splashed fingers, as seen in Fig. 9(c) (~9%, $D_m = [256 \pm 74]$ μm).

Figure 10 shows a TEM cross section located in the center of a large circular splat (similar to that shown in Fig. 9a). On the bright field image (Fig. 10a), the two arrows placed on each side of the cross section and marked with an ''I'' indicate the actual position of the NiCr/steel interface, since the contrast between these two phases is not distinct in the TEM image. The splat-substrate interface is more clearly distinguished on the EDS elemental maps (Fig. 10b and c). Consequently, the interface marked 1 is not the splat-substrate interface, rather grain boundaries within the steel substrate. The splat-substrate interface, indistinct on the bright field image (2), can be more clearly seen on the EDS elemental maps (Fig. 10b and c), and is slightly irregular in shape (3). The linescan L1 (Fig. 10f) shows that interdiffusion between Ni and Fe has occurred across the interface over a distance of ~250 nm (4). Consequently, localized substrate melting took place, followed by mixing or interdiffusion between the steel and the NiCr phase. The grains that have nucleated are relatively large (up to 10 μm in diameter) and appear to span the interface (5). This is consistent with a very slow cooling rate, and hence a low nucleation rate.

On the EDS elemental maps (Fig. 10d and e), chromium oxide can be observed at the splat-substrate interface (6): it appears as if it was present at this location upon splat formation, either from the oxidation of the substrate or the in-flight oxidation of the particle, and prevented substrate melting at this particular location, causing the irregularity observed in the interface shape. Chromium oxide is also observed on the outer surface of the splat as a thin, dense layer (7). This layer was too thin to be identified unambiguously by electron diffraction. However, as it has been discussed previously, Cr_2O_3 is the most likely oxide to have formed in such conditions.

Such interfacial features of intimate contact between splat and substrate, localized substrate melting, Ni-Fe interdiffusion and large grains having grown across the interface, were found on almost all along the main central sections of the large circular splats. This shows that strong metallurgical bonding can be achieved on most of the splat-substrate interfacial surface.

However, at the rim of the splat, curling up of the splat is observed. Figure 11 shows a FIB cross section prepared across the rim of a large circular splat. Poor contact between splat and substrate can be seen toward the splat periphery (1), as the splat has been lifted up above the substrate. This curling up phenomenon also occurred for the RSF splats (see section 3.1.4). A thin dense layer can be observed on the bottom surface of the splat in this area (2), which was identified using TEM as FeO. The formation of this phase is expected to be similar as for the oxides observed on the substrates sprayed at room temperature. Furthermore, the outer surface of the splat at its periphery displays an undulated morphology (3): it appears as if the flow of the NiCr was inhibited due to surface tension effects associated with the splat being in contact of the substrate.

The very good contact between splat and substrate and metallurgical bonding described for the large circular splats was less commonly found, however, for the irregularly shaped splats. Indeed, for instance, as shown in the TEM cross section presented in Fig. 12, located in the center of such a splat, the interface is, here, straight and distinct (1). The contact between splat and substrate may also be poor in some areas (2), with the presence of a thin chromium oxide layer (3) (possibly Cr_2O_3, however, the layer is too thin to obtain a clear electron diffraction pattern for unambiguous identification).

The small circular splats also displayed no evidence of substrate melting. Figure 13 displays a TEM cross section of such a splat, where the splat-substrate interface appears straight and distinct, with some fine voids (1) (Fig. 13a). Through EDS mapping a dense layer of chromium oxide

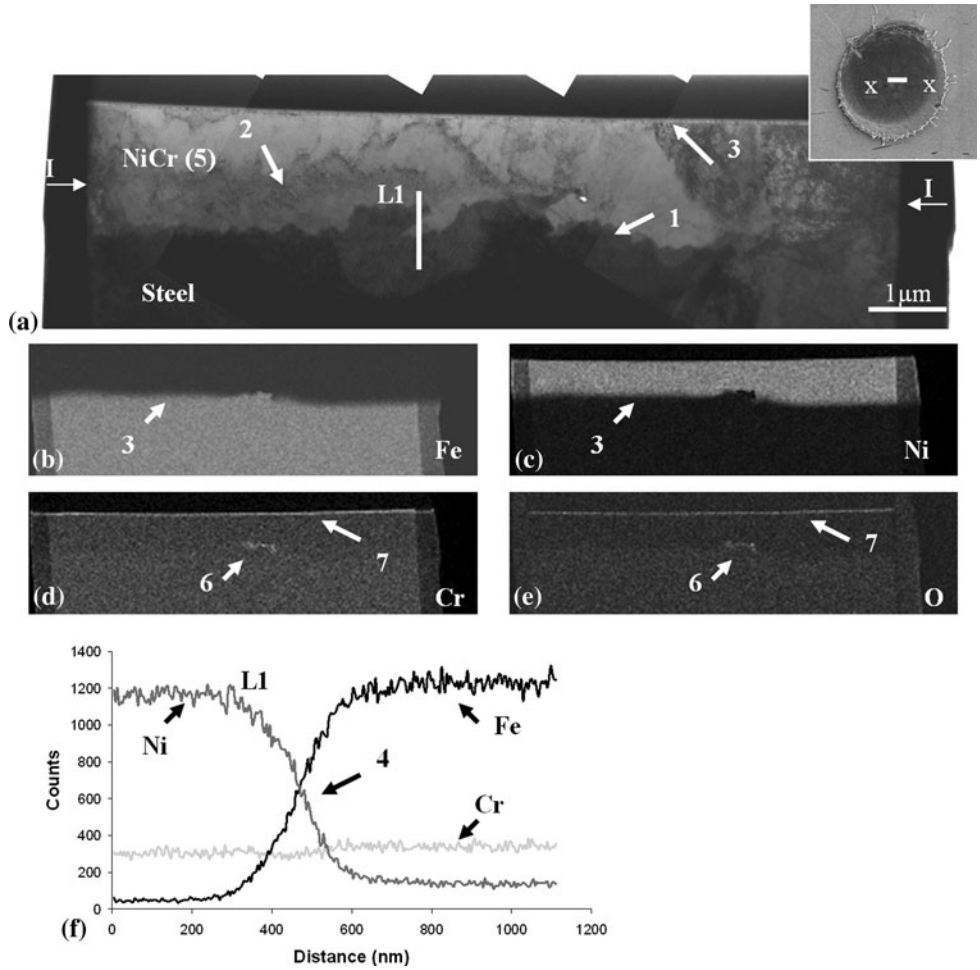

Fig. 10 TEM cross section made across the center of a large circular splat (see insert picture) found on SS_PH: (a) bright field image, EDS elemental maps for (b) Fe, (c) Ni, (d) Cr, (e) O, (f) EDS elemental linescan

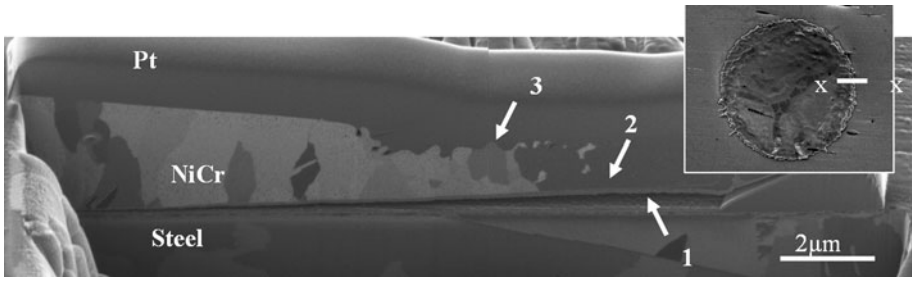

Fig. 11 FIB cross section made across the rim of a large circular splat (see insert picture) found on SS_PH

can be observed on the outer surface of the splat (2, Fig. 13d and e), and is most probably Cr_2O_3. It can be noted that these small splats are very thin (usually ~0.5 µm or less). Since their average diameter is ~37 µm, it can be calculated that the volume of NiCr in this splat is equivalent to a spherical particle of ~10 µm in diameter. By contrast, the diameters of the sprayed particles range from 5 to 45 µm, thus these small splats were formed from the smallest particles of the feedstock powder. Possibly because of their small size, their limited momentum (compared to the larger particles) and/or the thinner nature of the splats that formed may be responsible for the absence of signs of substrate melting. Indeed, limited momentum may translate to poorer contact upon impact between the particle and the substrate, limiting the heat transfer, and the thinner splats may transmit less heat to the substrate

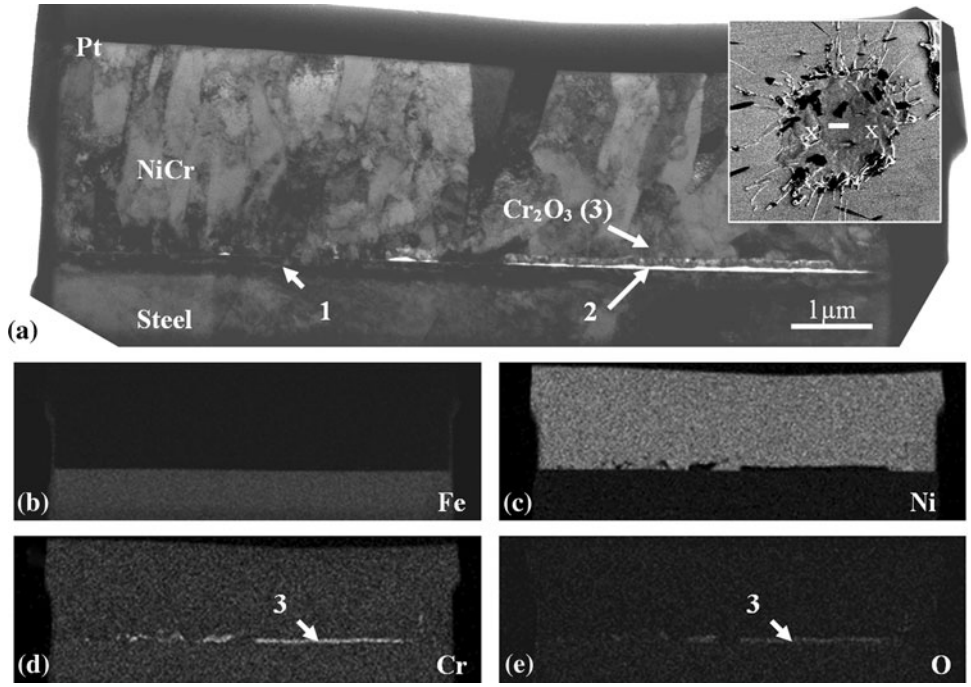

Fig. 12 TEM cross section made across the center of an irregularly shaped splat (see insert picture) found on SS_PH: (a) bright field image, EDS elemental maps for (b) Fe, (c) Ni, (d) Cr, (e) O

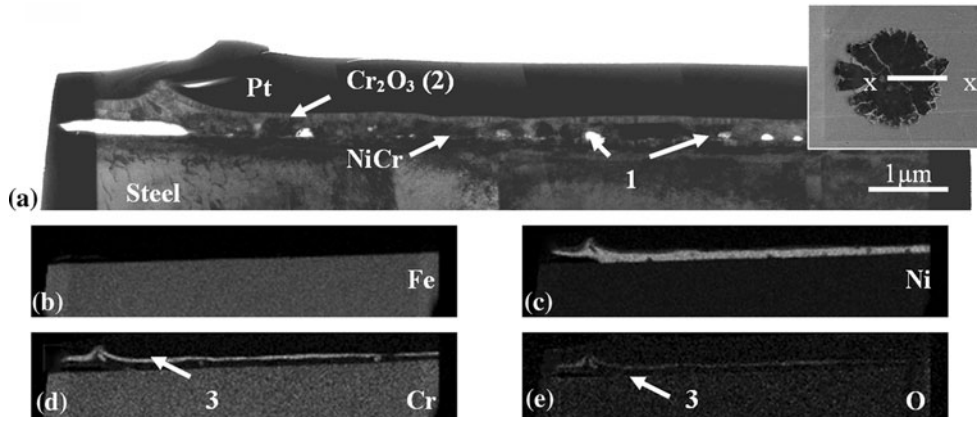

Fig. 13 TEM cross section across a small circular splat (see insert picture) found on SS_PH: (a) bright field image, EDS elemental maps for (b) Fe, (c) Ni, (d) Cr, (e) O

per unit of surface area. Some small splats may also arise from fragments splashed away from larger splats, as shown elsewhere (Ref 8, 43) such that, in the plasma spraying process, upon particle impact, vertical splashing occurred.

Finally, a few thick irregularly shaped splats were found on the specimen (the very few occurrences of these was such that they were not taken into account when statistically evaluating the splat population) such as shown in the inset image of Fig. 14: such splats appears to have formed from a NiCr particle that was only very partially molten. The FIB cross section made on this splat reveals a structure of almost equiaxed grains (1), finer than the expected grain structure of the NiCr particle (usually 3-8 μm), which may then originated from the partial melting and/or recrystallization of a NiCr particle from the feedstock powder upon heating and deformation upon impact. Other FIB cross sections of similar splats also showed the presence of fragments presenting a very similar grain structure reminiscent of the NiCr feedstock. Here, it can also be observed that the contact between the splat and the substrate is very poor (2). Moreover, a very finely grained layer can be seen on the under surface of the splat (3), possibly FeO as it is very commonly observed in such location (it should be noted that no TEM cross section could be made due to the excessive thickness of these splat to assist in identification of this phase).

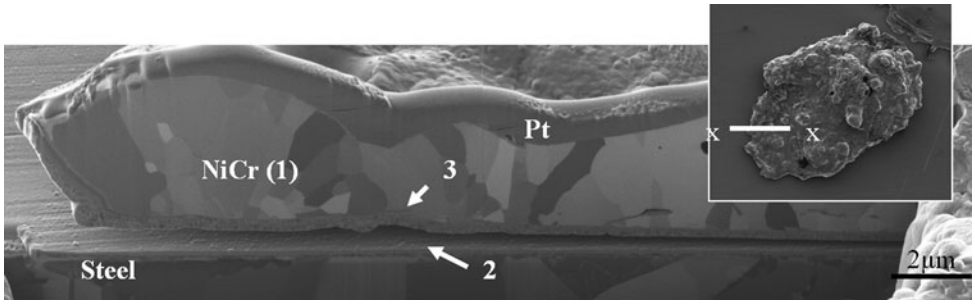

Fig. 14 FIB cross section of a partially melted splat found on SS_PH

3.2.2 Effects of Heating of the Substrate During Spraying on the Splat Morphology and Formation. Many studies have shown that heating a substrate during plasma spraying at a temperature above the transition temperature resulted in disk-shaped splats rather than irregularly shaped ones with many splashed fingers (Ref 3, 14-18). In the case observed here, the steel specimen was heated at the temperature of 350 °C during spraying, thus above the transition temperature of 337 °C that was determined by Fukumoto et al. (Ref 3) Consequently, the change observed in the shape of the splats, from very irregular with splashed fingers for the SS_P specimen to disk-shaped for the SS_PH specimen, was expected and the phenomena involved in such shift have already been widely discussed (Ref 3, 14-18).

On the other hand, additional phenomena were observed in the present study. Indeed, it was observed that substrate melting and interdiffusion between the splat and substrate occurred at a greater extent than for the non-heated specimen. Indeed, the observed depth of interdiffusion is usually ~150-250 nm for non-heated substrates, and ~200-300 nm for the heated substrates. Moreover, it appears that interdiffusion occurs on a larger proportion of the splat-substrate interface for the heated substrate. Indeed, the splats on these specimens present a much better contact with the substrate, as poor contact is observed only under the rim, compared to the many cases of poor contact observed for the non-heated substrates (under the rim and the splashed fingers of the RSF splats, almost all over the splat-substrate interface for the NSF splats, …). This may be explained, on one hand, by the absence (or limited amount) of gas released from the substrate. The heating of the substrate may also mean that the difference between the substrate temperature and the impacting splat is lower, and so the rate of heat removal across the interface will be slower. That is, the substrate is kept at a high temperature for longer. The suggestion of a slower cooling rate is, however, in disagreement with previous studies, notably the work of McDonald et al. (Ref 18), who suggested that heating the substrate during spraying would increase the cooling rate. The occurrence of substrate melting observed for the splats presented here may explain the different behavior.

Also, it was observed that the splats formed tended to be relatively thicker than for the ones on the non-heated specimen. This suggests that the heating may affect the wetting of the molten splat, causing it to spread less. The presence of undulations of the splat surface at the periphery also may come from the flow of the molten NiCr which was inhibited by the surface tension effects from the substrate. Alternatively, it may originate from the solidification of the bottom layers of the splat starting while the splat is still spreading, and thus slowing down the flow of NiCr on the top.

Concerning the more irregularly shaped splats, their formation was expected as the concept of transition temperature does not represent a precisely defined point above which all splats will be disk-shaped, but is rather an inflexion point representing the proportion of disk-shaped splats versus irregular ones (Ref 3). Thus, irregularly shaped splats will form, especially when heating the substrate at a temperature close to the transition one. Their process of formation should be similar to the irregularly shaped splats found on the non-heated specimens, for those splats not presenting evidence of substrate melting.

Furthermore, contrary to the non-heated specimens, the presence of many small splats, presumably formed from the smallest particle of the feedstock powder, was observed. A possible explanation may be that due to the improved wetting, these smaller particles, which do not adhere on the non-heated specimens may, because of their limited momentum, adhere in this instance. Furthermore, the fact that a few partially melted splats were found only on the SS_PH specimen may be explained by the improved adhesion induced by the heating of the substrate, as on the non-heated specimen they may just have not adhered to the substrate.

Finally, larger amounts of chromium oxide were found to form on the outer surface of the splat at this substrate temperature. A reason for this may be that splats, due to the heating, are kept a higher temperature longer and thus oxidation leading to the formation of Cr_2O_3 is more likely to occur. While more oxide may adversely affect some properties of the fully deposited, it is clear that heating of the substrate during spraying, by significantly reducing the splashing and increasing the occurrence and depth of substrate melting and mixing with the sprayed material, would then have a positive effect on the adhesion on the coating.

4. Conclusion

To conclude, the microstructural study of NiCr splats plasma sprayed on stainless steel led to the following observations:

- On both polished and polished and thermally treated substrates, sprayed at room temperature, a large proportion of the splats displayed a ring of splashed fingers. Toward their center, evidence of substrate melting and interdiffusion between NiCr and steel phases was found, showing metallurgical bonding. This was not found for the other types of splats.
- Heat treatment of the substrate prior to spraying led not only to a better wetting of NiCr on steel, thus thinner splats with a larger diameter, but also to a reduction of the occurrence of substrate melting.
- Heating the substrate during spraying resulted in the formation of a very large majority of disk-shaped splats with no, or very limited, splashing, and also substrate melting on a larger scale, thus a likelihood of improved adhesive strength of the fully deposited coating.

Acknowledgments

The authors acknowledge the Australian Research Council for provision of funding.

References

1. R.F. Bunshah, *Handbook of Hard Coatings. Deposition Technologies, Properties and Applications*, William Andrew Publishing/Noyes, Norwich, NY, 2001
2. M. Dorfman, Thermal Spray Basics, *Adv. Mater. Process.*, 2002, **160**, p 47-50
3. M. Fukumoto, M. Shiiba, H. Kaji, and T. Yasui, Three-Dimensional Transition Map of Flattening Behavior in the Thermal Spray Process, *Pure Appl. Chem.*, 2005, **77**(2), p 429-442
4. F. Otsubo, H. Era, and K. Kishitake, Interface Reaction Between Nickel-Base Self-Fluxing Alloy Coating and Steel Substrate, *J. Therm. Spray Technol.*, 2000, **9**(2), p 259-263
5. H. Du, J.H. Shin, and S.W. Lee, Study on Porosity of Plasma-Sprayed Coatings by Digital Image Analysis Method, *J. Therm. Spray Technol.*, 2005, **14**(4), p 453-461
6. J.M. Guilemany, J. Nutting, and M.J. Dougan, A Transmission Electron Microscopy Study of the Microstructures Present in Alumina Coatings Produced by Plasma Spraying, *J. Therm. Spray Technol.*, 1997, **6**(4), p 425-429
7. J. Cedelle, M. Vardelle, and P. Fauchais, Influence of Stainless Steel Substrate Preheating on Surface Topography and on Millimeter- and Micrometer-Sized Splat Formation, *Surf. Coat. Technol.*, 2006, **201**, p 1373-1382
8. J. Cedelle, M. Vardelle, B. Pateyron, and P. Fauchais, Investigation of Plasma Sprayed Coatings Formation by Visualization of Droplet Impact and Splashing on a Smooth Substrate, *Trans. Plasm. Sci.*, 2005, **33**(2), p 414-415
9. R. Dhiman, A.G. McDonald, and S. Chandra, Predicting Splat Morphology in a Thermal Spray Process, *Surf. Coat. Technol.*, 2007, **201**, p 7789-7801
10. R. Ghafouri-Azar, S. Shakeri, S. Chandra, and J. Mostaghimi, Interactions Between Molten Metal Droplets Impinging on a Solid Surface, *Int. J. Heat Mass Transf.*, 2003, **46**, p 1395-1407
11. S. Goutier, M. Vardelle, J.C. Labbe, and P. Fauchais, Alumina Splat Investigation: Visualization of Impact and Splat/Substrate Interface for Millimetre Sized Drops, *J. Therm. Spray Technol.*, 2010, **19**(1-2), p 49-55
12. L. Bianchi, A. Denoirjean, F. Blein, and P. Fauchais, Microstructural Investigation of Plasma-Sprayed Ceramic Splats, *Thin Solid Films*, 1997, **299**, p 125-135
13. S. Sampath and X. Jiang, Splat Formation and Microstructure Development During Plasma Spraying: Deposition Temperature Effect, *Mater. Sci. Eng. A*, 2001, **304-306**, p 144-150
14. H. Zhang, X.Y. Wang, L.L. Zheng, and X.Y. Jiang, Studies of Splat Morphology and Rapid Solidification During Thermal Spraying, *Int. J. Heat Mass Transf.*, 2001, **44**, p 4579-4592
15. C.-L. Li and J.-L. Li, Evaporated-Gas-induced Splashing Model for Splat Formation During Plasma Spraying, *Surf. Coat. Technol.*, 2004, **184**, p 13-23
16. H. Li, S. Costil, H.-L. Liao, C.-J. Li, M. Planche, and C. Coddet, Effects of Surface Conditions on the Flattening Behavior of Plasma Sprayed Cu Splats, *Surf. Coat. Technol.*, 2006, **200**, p 5435-5446
17. M. Fukumoto, E. Nishioka, and T. Matsubara, Flattening Solidification Behavior of a Metal Droplet on a Flat Substrate Surface Held at Various Temperatures, *Surf. Coat. Technol.*, 1999, **120-121**, p 131-137
18. A. McDonald, C. Moreau, and S. Chandra, Thermal Contact Resistance Between Plasma-Sprayed Particles and Flat Surfaces, *Int. J. Heat Mass Transf.*, 2007, **50**, p 1737-1749
19. M. Fukumoto, H. Nagai, and T. Yasui, Influence of Surface Character Change of Substrate due to Heating on Flattening Behavior of Thermal Sprayed Particles, *J. Therm. Spray Technol.*, 2006, **15**(4), p 759-764
20. L. Bianchi, A.C. Leger, M. Vardelle, A. Vardelle, and P. Fauchais, Splat Formation and Cooling of Plasma-Sprayed Zirconia, *Thin Solid Films*, 1997, **305**, p 35-47
21. T. Chraska and A.H. King, Effect of Different Substrate Conditions upon Interface with Plasma Sprayed Zirconia—A TEM Study, *Surf. Coat. Technol.*, 2002, **157**, p 238-246
22. Z.G. Feng, M. Domaszewski, G. Montavon, and C. Coddet, Finite Element Analysis of Effect of Substrate Surface Roughness on Liquid Droplet Impact and Flattening Process, *J. Therm. Spray Technol.*, 2002, **11**(1), p 62-68
23. A.A. Syed, A. Denoirjean, B. Hannoyer, P. Fauchais, P. Denoirjean, A.A. Khan, and J.C. Labbe, Influence of Substrate Surface Conditions on the Plasma Sprayed Ceramic and Metallic Particles Flattening, *Surf. Coat. Technol.*, 2005, **200**, p 2317-2331
24. S. Kitahara and A. Hasui, A Study of the Bonding Mechanism of Sprayed Coatings, *J. Vac. Sci. Technol.*, 1974, **11**(4), p 747-753
25. L. Li, X.Y. Wang, G. Wei, A. Vaidya, H. Zhang, and S. Sampath, Substrate Melting During Thermal Splat Quenching, *Thin Solid Films*, 2004, **468**, p 113-119
26. H.-D. Steffens, B. Wielage, and J. Drozak, Interface Phenomena and Bonding Mechanism of Thermally-Sprayed Metal and Ceramic Composites, *Surf. Coat. Technol.*, 1991, **45**, p 299-308
27. C.-J. Li and J.-L. Li, Transient Contact Pressure During Flattening of Thermal Spray Droplet and its Effect on Splat Formation, *J. Therm. Spray Technol.*, 2004, **13**(2), p 229-238
28. L. Li, A. Vaidya, S. Sampath, H. Xiong, and L. Zheng, Particle Characterization and Splat Formation of Plasma Sprayed Zirconia, *J. Therm. Spray Technol.*, 2006, **15**(1), p 97-105
29. J. Mostaghimi and S. Chandra, Splat Formation in Plasma-Spray Coating Process, *Pure Appl. Chem.*, 2002, **74**(3), p 441-445
30. M. Pasandideh-Fard, S. Chandra, and J. Mostaghimi, A Three-Dimensional Model of Droplet Impact and Solidification, *Int. J. Heat Mass Transf.*, 2002, **45**, p 2229-2242
31. M.E. Aalamialeagha, S.J. Harris, and M. Emamighomi, Influence of the HVOF Spraying Process on the Microstructure and Corrosion Behaviours of Ni-20%Cr Coatings, *J. Mater. Sci.*, 2003, **38**, p 4587-4596
32. S. Brossard, P.R. Munroe, A.T.T. Tran, and M.M. Hyland, Study of the Effects of Surface Chemistry on Splat Formation for Plasma Sprayed NiCr onto Stainless Steel Substrates, *Surf. Coat. Technol.*, 2009, **204**(9-10), p 1599-1607
33. A.T.T. Tran, M.M. Hyland, T. Qiu, B. Withy, and B.J. James, Effect of Surface Chemistry on Splat Formation During Plasma Spraying, *J. Therm. Spray Technol.*, 2008, **17**(5-6), p 637-645

34. S. Brossard, P.R. Munroe, A.T.T. Tran, and M.M. Hyland, Study of the Microstructure of NiCr Splats Plasma Sprayed on Stainless Steel by TEM, *Surf. Coat. Technol.*, 2009, **204**(9-10), p 1608-1615
35. P.R. Munroe, The Application of Focused Ion Beam Microscopy in the Material Sciences, *Mater. Charact.*, 2009, **60**, p 2-13
36. A.T.T. Tran and M.M. Hyland, The Role of Substrate Surface Chemistry on Splat Formation During Plasma Spray Deposition by Experiments and Simulations, *J. Therm. Spray Technol.*, 2010, **19**(1-2), p 11-23
37. MatWeb, Material Property Data, 2008 11/11/2008; Available from: http://www.matweb.com/
38. S. B. Newcomb, ''A Microstructural Study of the Oxidation of Ni-Cr Steels in Air and in CO-CO_2'', PhD Thesis, University of Cambridge, 1982
39. G.C. Allen, J.M. Dyke, S.J. Harris, and A. Morries, A Surface Study of the Oxidation of Type 304L Stainless Steel at 600 K in Air, *Oxid. Met.*, 1987, **29**(5/6), p 1988
40. N.S. McIntyre, T.C. Chan, and C. Chen, Characterization of Oxide Structures Formed on Nickel-Chromium Alloy During Low Pressure Oxidation at 500-600 °C, *Oxid. Met.*, 1990, **33**(5/6), p 457-479
41. J. Stringer, B.A. Wilcox, and R.I. Jaffee, The High-Temperature Oxidation of Nickel-20 wt% Chromium Alloys Containing Dispersed Oxide Phases, *Oxid. Met.*, 1972, **5**(1), p 11-47
42. X.Y. Jiang, Y. Wan, H. Herman, and S. Sampath, Role of Condensate and Adsorbates on Substrate Surface on Fragmentation of Impinging Molten Droplets During Thermal Spray, *Thin Solid Films*, 2001, **385**, p 132-141
43. C. Escure, M. Vardelle, and P. Fauchais, Experimental and Theoretical Study of the Impact of Alumina Droplets on Cold and Hot Substrates, *Plasma. Chem. Plasma Process.*, 2003, **23**(2), p 185-221
44. M. Xue, S. Chandra, and J. Mostaghimi, Investigation of Splat Curling up in Thermal Spray Coatings, *J. Therm. Spray Technol.*, 2006, **15**(4), p 531-536